Use of Complex Impedance To Monitor the Progress of Reactions in Epoxy/Amine Model Systems

Jovan Mijovic* and C. F. Winnie Yee

Department of Chemical Engineering, Polytechnic University, Six MetroTech Center, Brooklyn, New York 11201

Received March 31, 1994; Revised Manuscript Received September 6, 1994®

ABSTRACT: Reactions in a model epoxy/amine system at elevated temperatures were investigated by dielectric measurements. Experiments were conducted in a frequency range where polarization by charge migration is the dominant mechanism. It was shown how the complex impedance can be utilized as an effective multifaceted diagnostic tool for monitoring the progress of reactions.

I. Introduction

A vigorous research activity has unravelled in recent years regarding the fundamental and applied aspects of dielectric properties of polymeric materials. Fundamental dielectric investigations yield a wealth of information about molecular motions and relaxation processes, while a strong interest in the applied research reflects the growing use of polymers in coatings, encapsulants, electronic interconnect devices, printed board circuitry, microwave assemblies for radars, batteries, and fuel cells, etc. An extensive literature on dielectric behavior of polymers has been accumulated in several books and key reviews.[1-9]

When an electric field is applied across a parallel-plate capacitor containing a dielectric, various atomic and molecular charges that are present in the dielectric are displaced from their equilibrium positions and the material is said to be polarized. Different polarization mechanisms can occur, including dipole orientation, extrinsic free change migration (e.g., impurities), intrinsic charge migration (e.g., protonic via hydrogen bonds), electrode polarization, and, in heterogeneous or composite systems, the Maxwell–Wagner–Sillars interfacial polarization. The contributions of atomic and electronic charges, which occur at frequencies above 100 GHz, are considered to be instantaneous in the dielectric studies of polymers.

In general, contributions to the overall dielectric polarization come from the moieties or particles whose relaxation times are faster than the time scale of the applied signal. This important fundamental characteristic enables one to distinguish between various polarization mechanisms on the basis of their different frequency dependencies. The remarkable frequency range available in the dielectric measurements, from as low as 10^{-5} Hz to as high as 10^{11} Hz, makes it possible to single out a desired frequency interval and relate the corresponding dielectric response to a specific polarization mechanism. In this paper, we shall focus our attention on the frequency range in which the contributions of migrating charge carriers dominate the dielectric response.

The above-cited information on the dielectric behavior of polymers pertains almost exclusively to nonreactive systems. The application of dielectric measurements to in-situ real-time monitoring of **the progress of reactions** in polymer-forming and non-polymer-forming systems has a much more recent origin; a notable example is a strong research activity in the last 10 years that led to the development of experimental methods to calculate ionic conductivity from the measured dielectric loss and use it to control the processing of polymers and composites. It should be emphasized, however, that neither the conductivity mechanism nor the fundamental relationships between the dielectric response and the two principal phenomena that characterize thermoset processing, gelation and vitrification, have been established. A review of this subject has been recently published.[10]

In this paper we shall use some of our recent experimental and analytical results to present an elegant methodology for the analysis of dielectric properties of reactive organic systems. At the heart of our approach is the use of real and imaginary components of the complex impedance to monitor the progress of reactions. To the best of our knowledge, no such study has been reported in the literature. Changes in the complex impedance in the course of the model reaction studied herein are a measure of variations in the contributions of migrating charges to the overall polarization.

The principal objective of this paper is to describe how complex impedance, obtained from dielectric measurements, can be used as an effective diagnostic tool for in-situ real-time investigation of reactive systems.

II. Experimental Section

Materials. The reactive model system used in this study consisted of 1,2-epoxy-3-phenoxypropane and aniline. The former compound is also known as phenyl glycidyl ether, or PGE, and will be referred to in the text by this acronym.

Sample Preparation. The stoichiometric amounts of aniline and PGE were mixed at room temperature and immediately tested at a series of selected isothermal temperatures in the range between 90 and 120 °C.

Technique. Dielectric measurements were performed on a Hewlett–Packard Model 4284A precision LCR meter, operable in the frequency range from 20 Hz to 1 MHz. The low limit levels of voltage and current of the test signal are 5 mV and 5 μA, respectively. Our equipment was modified by the addition of a temperature-controlled chamber and was interfaced to peripherals via NI's IEEE 488.2 bus. At each frequency, a low-voltage ac excitation wave was applied to the metallic electrodes and the overall impedance measured. The excitation frequency was varied from the maximum of 10^6 Hz to a minimum value that depended on the time and temperature of the measurement. Ten frequencies were swept in each measurement. For each reaction time, five steps were taken at each of the 10 frequencies. The time required to complete a frequency sweep depended on the lowest value of frequency (f_{min}) employed during the run. The time scale of the experi-

* To whom correspondence should be addressed.

® Abstract published in *Advance ACS Abstracts,* November 1, 1994.

0024-9297/94/2227-7287$04.50/0

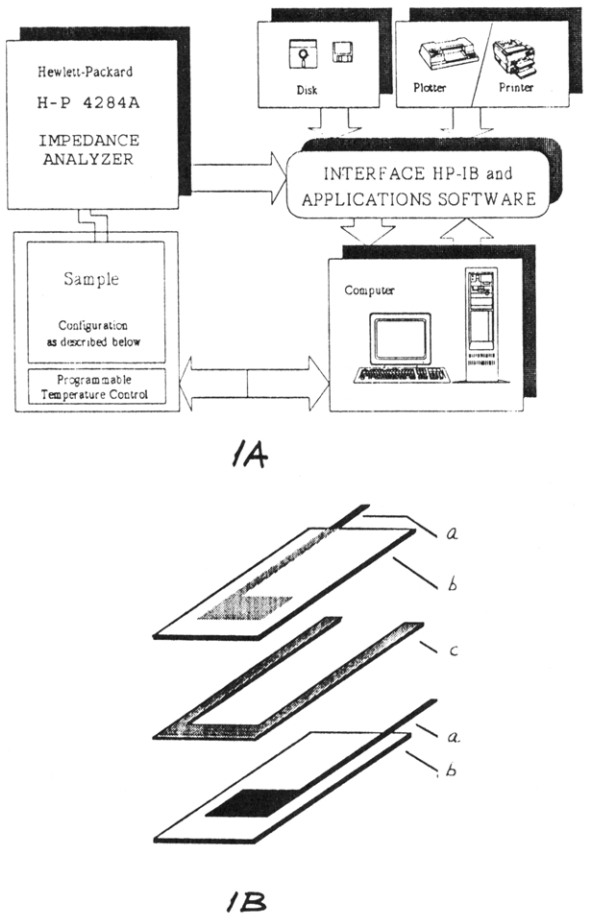

Figure 1. (A) Schematic of the experimental setup for dielectric measurements. (B) Schematic of the measuring cell: (a) electrode, (b) glass, (c) Teflon spacer.

ment was negligible in comparison with the time scale of the changes in the reactive system; hence, each measurement could be taken to represent an isostructural state. A schematic diagram of the experimental setup is shown in Figure 1A. The measuring cell, depicted in Figure 1B, consisted of two glass slides (Fischer Scientific's Premium Microscope Slides, measuring 25 × 75 × 1 mm), separated by a 1.6-mm-thick Teflon shim. Teflon was attached to glass on both sides using a special silicone adhesive transfer tape (Specialty Tapes' CW-14HT High Temperature Silicone Transfer Tape). Thin aluminum electrodes, with surface area of 4 cm^2, were placed on each glass plate. The cell constant, $K = S/L$, was equal to 25. Temperature was monitored with an embedded sensor adjacent to the measuring cell. The temperature inside the sample was verified in a series of calibration runs using Luxtron's Model 750 fluorooptic temperature probe. During tests, the cell was vertically held to allow resin shrinkage (less than 2%) without altering the distance between electrodes, thus avoiding its effect on the measurement.

III. Results and Discussion

Reaction Scheme. At the conditions of this study, the reaction between PGE and aniline occurs in two consecutive steps shown in Figure 2. An epoxy group reacts with a primary amine to form a secondary amine which, in turn, reacts with another epoxy to form a tertiary amine. No etherification was observed. This reaction scheme is intended only as an illustration of the events on the molecular level; the molecular mechanism and the chemorheological aspects of this reaction will not be discussed here, and the interested reader is referred to the pertinent literature (e.g., ref 11). The rationale in choosing this system was based upon the lack of evolution of small molecules during reactions, its importance in modeling of cure of multifunctional epoxy resins, and our considerable experience with the chemorheological behavior of this generic group of materials.

Conductivity due to Migrating Charges. As pointed out in the excellent account by Jonscher,[12] dielectric response of a nonreactive material may be represented by two frequency-dependent parameters which define the real and imaginary components of any one of the following three parameters: (1) the complex dielectric constant (ϵ^*); (2) the complex admittance (Y^*); or (3) the complex impedance (Z^*). Our investigations hitherto, with non-polymer-forming and polymer-forming systems alike, have shown that the complex impedance varies in a systematic manner during reaction and is superior when compared to other parameters in describing the dielectric response of reactive systems due to polarization by migrating charges. The origin of migrating charges is described below. From the measured impedance we evaluate the corresponding resistance and calculate the conductivity and/or resistivity due to migrating charges, either of which can then be used as an indicator of the progress of reactions. The contribution of migrating charges to the overall polarization varies during reaction as a consequence of physical and chemical changes in the reactive system, which continually alter the interactions between these charges and the host matrix.

We shall now describe the principal features of experimental and analytical evaluation of the complex impedance during reaction and their relevance to the development of models based on equivalent circuits. The measured dielectric response will be related to the general physical nature of the process; albeit no attempts will be made to elucidate the molecular nature of conductivity or to seek fundamental relationships between the dielectric response and the phenomena of gelation and vitrification. These important questions remain unsolved, as exemplified by a spirited comment-

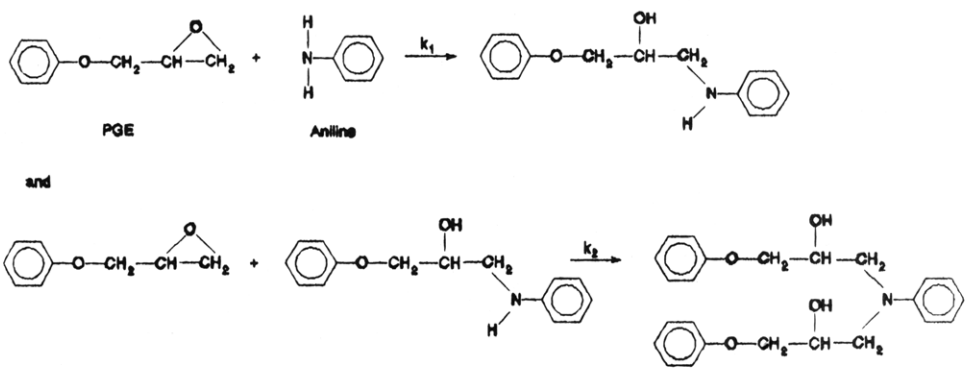

Figure 2. Chemical reactions in the PGE/aniline system.

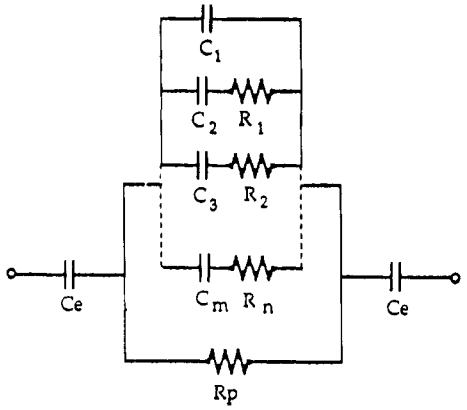

Figure 3. General equivalent circuit model of a polymer with contributions to dielectric polarization from electrode blocking layers, migrating charges, and dipoles.

and-rebuttal exchange between two prominent scientists, which recently appeared in this journal.[13,14] In the vast majority of the published reports on cure of thermosets, conductivity is interpreted as resulting from the "ionic impurities". This assertion is routinely invoked, yet, amazingly, no fundamental evidence to support this tenet has been put forward. The fact is that ionic impurities represent but one of the contributors to the measured conductivity. For that very reason we prefer the use of more general terms "migrating charges" or "migrating charge carriers", which are more appropriate as they encompass the contributions to conductivity from both extrinsic and intrinsic sources. The former group includes, for instance, the "familiar" ionic impurities present as remnants from the various steps in synthesis, as well as the metallic ions that emanate from the electrodes, as shown in some recent studies (ref 6 and references therein). Further complications arise in the instances where specific interaction between extrinsic charges and the host matrix can develop. There are a variety of mechanisms that can contribute to the intrinsic conductivity by migrating charge carriers. In general, these depend on the inherent chemical characteristics of the formulation components and include proton transfer via hydrogen bonding as well as various inductive and resonance effects. Although the molecular mechanism of conductivity will not be discussed in this paper, we would like to emphasize that, in the model system studied here, both extrinsic and intrinsic migrating charges have contributed to the measured conductivity. The effect of extrinsic charges was confirmed by first measuring the initial concentration of sodium (Na^+) using atomic absorption (the results was 1.79 ppm) and then doping the system with lithium trifluoromethanesulfonate ($LiCF_3SO_3$). The contribution of intrinsic charges was established from a series of measurements with increasing concentration of aniline. In both instances, an increase in conductivity was observed.

Modeling Concepts. The models of dielectric behavior are based on series and/or parallel combinations of resistances (R) and capacitances (C) that can account for the contribution of all active mechanisms to the overall dielectric polarization. In-depth accounts of the fundamental aspects of equivalent circuit modeling are available in the literature,[15-18] but, as a rule, they do not address the subject of reactive organic systems. Modeling of reactive polymers with contributions from various polarization mechanisms has been discussed in recent papers from our laboratory[19,20] and will not be restated here; instead, only the salient features of our approach will be highlighted. In the most general case, the equivalent circuit model of a polymer characterized by the presence of electrode polarization (C_e), conductivity due to migrating charges (R_p), and dipolar relaxations with a distribution of relaxation times (C_iR_{i-1}) is shown in Figure 3. Solving the equivalent circuit of Figure 3 for the real and imaginary components of the complex impedance, we obtain:

$$Z' = \frac{R_p[1 - R_p\tau C_1\omega^2 + \tau\omega^2(R_pC_1 + R_pC_2 + \tau)]}{(1 - R_p\tau\omega^2C_1)^2 + \omega^2(R_pC_1 + R_pC_2 + \tau)^2} \quad (1a)$$

$$Z'' = \frac{R_p[\omega(R_pC_1 + R_pC_2 + \tau) - \omega\tau(1 - R_p\tau\omega^2C_1)]}{(1 - R_p\tau\omega^2C_1)^2 + \omega^2(R_pC_1 + R_pC_2 + \tau)^2} + \frac{2}{C_e\omega} \quad (1b)$$

where $C_1 = \epsilon_u C_0$, $C_2 = (\epsilon_r - \epsilon_u)\, C_0$, and $\tau = RC_2$.

In this paper, a considerably simpler model was used, since we focused our attention on the polarization by migrating charge carriers only. The said simplification was made possible by operating above the frequencies where the electrode polarization occurs and below the frequencies where dipolar relaxations occur. A clear separation of the contributions of electrode polarization, migrating charges, and dipoles, in terms of their frequency dependencies, is readily accomplished with the complex impedance data, in the manner described below.

Electrode polarization (or interfacial polarization, in multiphase systems) is caused by the entrapment of charges at electrodes (or interfaces) which alters the electric field and gives rise to an increase in the capacitance of the sample. If not properly account for, erroneously high values of the dielectric constant are calculated. Although electrode polarization generally occurs at lower frequencies, its effect in reactive systems, depending on the extent of reaction and temperature, can persist at frequencies up to 10^2 Hz, or even higher. The manner in which we utilize the complex impedance data to separate the effects of electrode polarization and conductivity due to migrating charges is detailed below. Dipolar relaxations, on the other hand, for most low molecular weight organic polar molecules occur at frequencies in the megahertz and low gigahertz (GHz) range. This is exemplified in Table 1, where we list relaxation times (τ) in picoseconds (ps) and the corresponding frequencies (f) in GHz for several organic molecules at room temperature. At the conditions of this study, dipolar loss does not occur in the frequency range dominated by the migration of free charges.

Table 1. Relaxation Times and Corresponding Frequencies of Some Polar Molecules

material	τ (ps)	f (GHz)	material	τ (ps)	f (GHz)
acetonitrile	3.3	48	methanol	48	3
water	7.9	22	*N*-methylformamide	123	1.3
tetramethylurea	31	5	ethanol	130	1.2
benzonitrile	38	4	1-propanol	390	0.4

The resistance and capacitance of an equivalent circuit have the following physical meaning in our case. Migration of extrinsic and/or intrinsic charges is a dissipative process (it contributes to the dielectric loss but not to the dielectric permittivity) and is represented by the resistance. The capacitance, on the other hand,

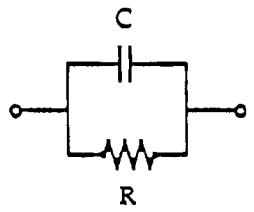

Figure 4. $R-C$ parallel equivalent circuit.

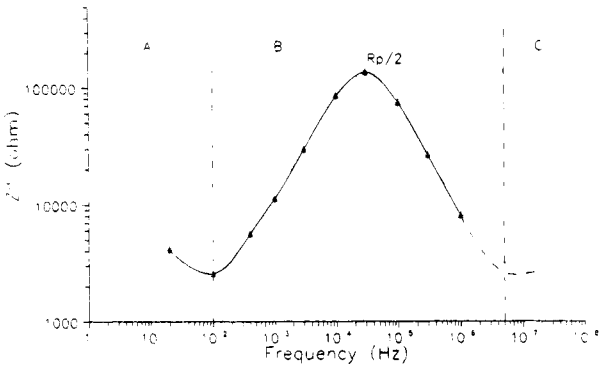

Figure 5. Imaginary component of the complex impedance as a function of frequency for a PGE/aniline sample reacted at 100 °C for 70 min.

measures the overall ability of our dielectric material to store the electric field. A single resistance that encompasses the dissipative contribution of all migrating charges, extrinsic and/or intrinsic alike, is sufficient in the model, since the dissipative contributions due to electrode polarization and dipolar relaxations fall outside the frequency range utilized in our analysis. Thus an $R-C$ parallel circuit of Figure 4, its simplicity notwithstanding, represents an adequate phenomenological model of the dielectric response of our system at the frequencies investigated in this study.

The formalism outlined below is generally applicable to the studies of conductivity by migrating charge carriers and is not conditioned by the underlying molecular mechanism. The total impedance of an $R-C$ parallel circuit is given as the inverse of the sum of contributions from capacitance and resistance:

$$Z = [1/R + j\omega C]^{-1} \tag{2}$$

By expressing the complex impedance in terms of its real and imaginary components, we obtain:

$$Z = Z' - jZ'' \tag{3a}$$

$$Z' = \frac{R}{1 + \omega^2 C^2 R^2} \tag{3b}$$

$$Z'' = \frac{\omega C R^2}{1 + \omega^2 C^2 R^2} \tag{3c}$$

Methods for Calculation of Impedance and Circuit Parameters. Quantitative evaluation of the circuit parameters can be carried out by using our experimental data in conjunction with one of the three representations described below.

Method 1. The first representation is based on the plots of imaginary impedance (Z'') as a function of frequency. An example of such a plot for the PGE/aniline system, reacted at 100 °C for 70 min, is shown in Figure 5. From the simultaneous high-preformance liquid chromatography (HPLC) study,[11] the extent of reaction at that point was determined to be approximately 20%. Three zones, roughly partitioned by frequencies f_1 and f_2, are readily distinguishable in Figure 5: zone A, where electrode polarization dominates the dielectric response; zone B, which was singled out in this study and where dissipative effects caused by charge migrations play the major role; zone C, where contributions from dipolar relaxations prevail. As discussed earlier in the text, at low frequencies, below ca. 10^2 Hz in this case, the capacitance of the electrode blocking layers is known to contribute strongly to the overall polarization. Therefore, in zone B of Figure 5, the dielectric signal is not affected by either electrode polarization or dipolar relaxations and, in the frequency range, the general equivalent circuit of Figure 3 reverts to a simple $R-C$ parallel model of Figure 4, whose imaginary impedance is described by eq 3c. Taking a derivative of Z'' with respect to the angular frequency, we get:

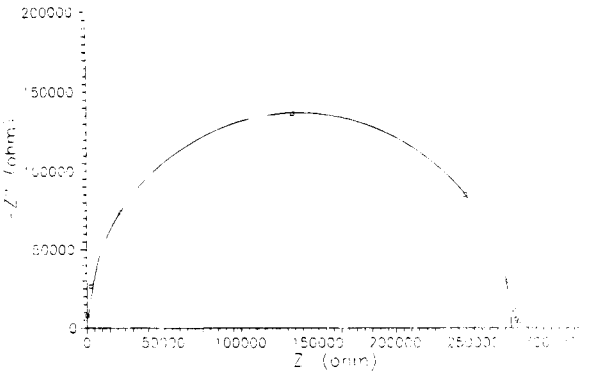

Figure 6. Nyquist plot of imaginary vs real component of the complex dielectric constant for a PGE/aniline sample reacted at 100 °C for 70 min.

$$\frac{dZ''}{d\omega} = \frac{CR_p^2(1 - \omega^2 R_p^2 C^2)}{(1 + \omega^2 R_p^2 C^2)} \tag{4}$$

Equation 4 is equal to zero when the following condition is met:

$$\omega = 1/R_p C \tag{5}$$

By combining eqs 4 and 5, we obtain:

$$Z_{max} = R_p/2 \tag{6}$$

and thus the unknown resistance R is obtained directly from Z''_{max}. From Figure 5, the calculated resistance was 273 kΩ.

Method 2. The second representation is based on the Nyquist plots of the imaginary (Z'') component of the complex impedance versus its real counterpart (Z'). An example of the Nyquist plot from the same PGE/aniline system, reacted at 100 °C for 70 min, is shown in Figure 6. An $R-C$ parallel equivalent circuit gives a semicircle in the Nyquist complex plane. The value of the resistance is obtained from the intersection of the semicircle and the Z' axis, as indicated in Figure 6. The value of the capacitance is calculated from the Nyquist plot using the following equation:

$$C = \frac{1}{2\pi f_{Z''_{max}} R} \tag{7}$$

For the system of Figure 6, the calculated values of

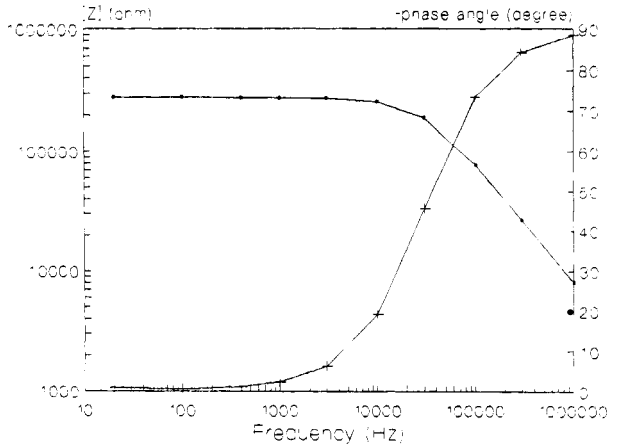

Figure 7. Bode plot of absolute impedance as a function of frequency for a PGE/aniline sample reacted at 100 °C for 70 min.

resistance and capacitance were 278 kΩ and 19.1 pF, respectively.

Method 3. The third representation of the complex impedance consists in plotting its absolute value, $[Z]$, where $[Z] = \{(Z')^2 + (Z'')^2\}$, as a function of the logarithm of frequency. This is known as the Bode plot. Its characteristic shape is shown in Figure 7 for the same PGE/aniline system (100 °C/70 min). The value of resistance is obtained from the intersection of the extrapolated frequency-independent horizontal line and the log $[Z]$ axis. At higher frequencies, the dielectric response is purely capacitive; impedance is inversely proportional to frequency, giving a straight line with a slope of −1. The value of capacitance is calculated from the following equation:

$$C = \frac{1}{2\pi f_t Z_t} \tag{8}$$

For the system of Figure 7, the calculated values of resistance and capacitance were 278 kΩ and 19.8 pF, respectively. As expected, the values of capacitance and resistance calculated by the three methods described above are identical.

The resistance calculated by any one of the methods described above represents the dissipative contribution to the dielectric polarization from all migrating charges. An apparent conductivity (σ) and/or resistivity (ϱ) due to migrating charges can be calculated from the following equation:

$$\sigma = 1/\varrho = L/RS \tag{9}$$

where S/L denotes the cell constant.

Use of Impedance To Monitor the Progress of Reactions. Let us now revert our attention to the evaluation of changes in the complex impedance **during reactions** using the three representations described above. Since each frequency sweep, as established earlier, involves an isostructural state, we conducted impedance measurements at selected time intervals during reaction. Regardless of which representation of data was chosen, the variation in impedance during reaction was systematic, extremely reproducible, and reliable. In Figures 8–11 we show the plots of imaginary impedance as a function of frequency, with reaction time as a parameter, for isothermal runs at 90, 100, 110, and 120 °C. Various interesting observations were made. We first point out the observed increase in Z'' with decreasing frequency, which is more pronounced

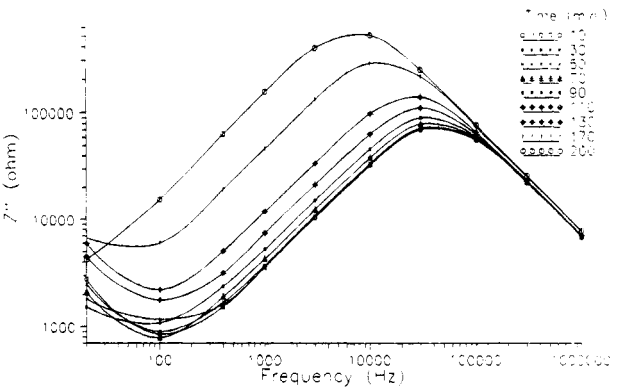

Figure 8. Imaginary component of the complex impedance as a function of frequency, with reaction time as a parameter, for a PGE/aniline sample reacted at 90 °C.

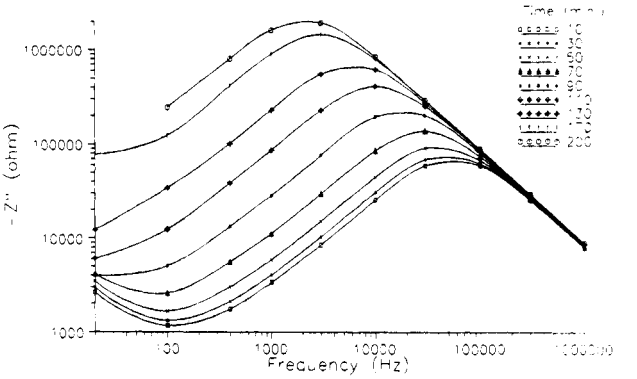

Figure 9. Imaginary component of the complex impedance as a function of frequency, with reaction time as a parameter, for a PGE/aniline sample reacted at 100 °C.

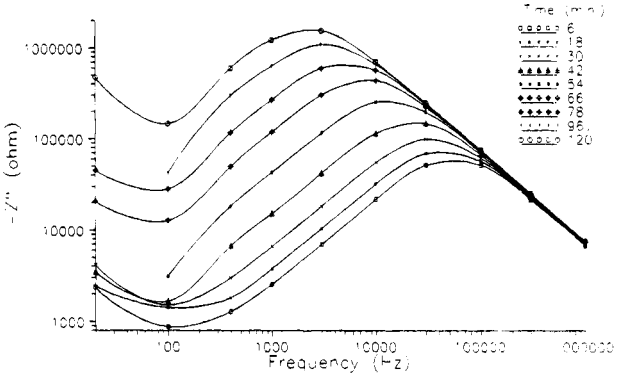

Figure 10. Imaginary component of the complex impedance as a function of frequency, with reaction time as a parameter, for a PGE/aniline sample reacted at 110 °C.

at short reaction times. This upward trend in Z'' marks the entrance into zone A of Figure 5 and is caused by the effect of electrode blocking layers. Importantly, however, the observed phenomenon does not overlap, and hence interfere, with the values of Z'' in zone B dominated by the dissipative contribution of migrating charges. The value of resistance calculated from eq 9 is therefore a true measure of the dissipative character of migrating charges. Our results clearly stress the necessity of data collection over a wide frequency range if one were to distinguish between different polarization mechanisms, a practice all too often overlooked in the literature.

Further, we note that (1) the value of maximum imaginary impedance increases and simultaneously shifts to lower frequency during reaction at a given temperature and (2) at a given reaction time the

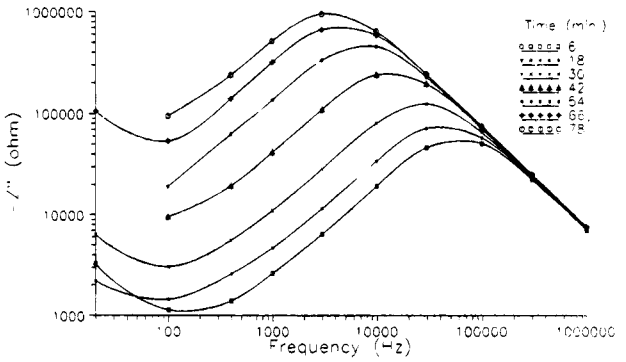

Figure 11. Imaginary component of the complex impedance as a function of frequency, with reaction time as a parameter, for a PGE/aniline sample reacted at 120 °C.

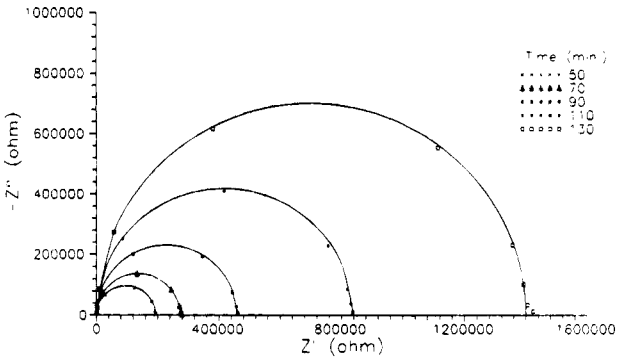

Figure 12. Nyquist plot of imaginary vs real component of the complex dielectric constant for a PGE/aniline sample reacted at 100 °C, with reaction time as a parameter.

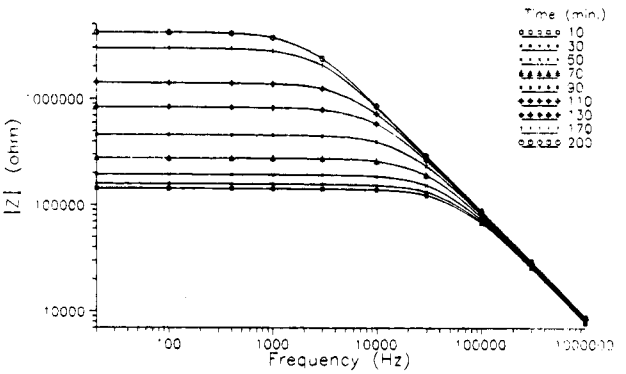

Figure 13. Bode plot of absolute impedance as a function of frequency for a PGE/aniline sample reacted at 100 °C, with reaction time as a parameter.

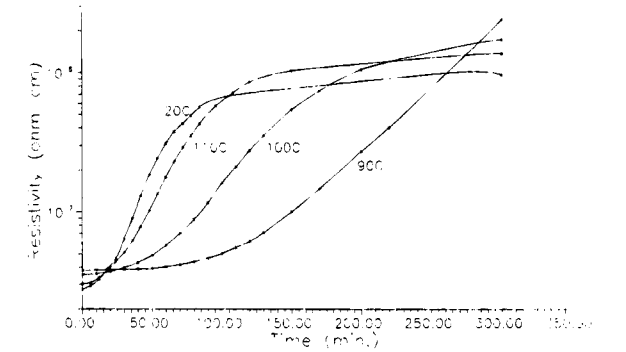

Figure 14. Resistivity due to migrating charges as a function of reaction time, with reaction temperature as a parameter.

maximum imaginary impedance decreases and simultaneously shifts to higher frequency with increasing temperature. These observations can be rationalized by considering the effect that the chemorheology of the reactive mixture has on the mobility of migrating charges and the nature of their interactions with the continually changing host matrix. Fundamental aspects of those issues are currently under investigation in our laboratory.

In Figure 12 we show the Nyguist plots generated at different times during the reaction between PGE and aniline at 100 °C. A semicircular shape of the plot is preserved during reaction, while its radius increases. The intersection of the low-frequency data with the Z' axis at its far end yields the value of resistance which, as expected, increases with reaction time. At the high frequency end, all plots extrapolate to the origin.

The Bode plots of absolute impedance as a function of log frequency constructed for various times during the PGE/aniline reaction at 100 °C are displayed in Figure 13. The frequency-independent horizontal line, from which the resistance is calculated, shifts upward, i.e., to higher resistance, during the reaction. The capacitive response, represented by the straight line of slope −1, extends during reaction to lower frequency and shifts, very slightly, to lower capacitance. The frequency of the transition point between capacitive and resistive response in the Bode plot corresponds to that of the maximum imaginary impedance in Figure 9.

The most striking features of each representation of the complex impedance of reactive systems are the systematic variation and superb reproducibility of the measured data. Utilizing the data of Figures 8−13 in conjunction with any one of the three methods of analysis, we can calculate first resistance and then, from eq 9, resistivity due to migrating charges at any time and temperature in the course of reaction. In Figure 14, we show the calculated resistivity as a function of time for PGE/aniline reactions at 90, 100, 110, and 120 °C. As expected, initial resistivity decreases as the temperature is increased. During the course of reaction, an S-shaped curve was observed at each temperature, characterized by an initial increase in resistivity and the subsequent leveling off to an asymptotic value. The resulting behavior bears a qualitative resemblance to the trend observed with the extent of reaction. In fact, the change of normalized resistivity during reaction mimics that of the extent of reaction obtained from calorimetric measurements, and a comparison between the two is useful. This analogy has been noted and exploited in empirical fashion by several researchers (e.g., ref 10 and references therein). In this study, we have selected an equation first reported by Keinle and Race[21] and later successfully utilized by Nass and Seferis,[22] which is of the following general form:

$$\alpha = A \log \varrho + B \tag{10}$$

Constants A and B are determined from the following boundary conditions

$$t = 0; \quad \alpha = 0; \quad \varrho = \varrho_0 \tag{11a}$$

and

$$t \to \infty; \quad \alpha = \alpha_m; \quad \varrho = \varrho_m \tag{11b}$$

where α_m depicts the maximum value of the extent of reaction attainable in cross-linking systems as a result of vitrification.[23] Combining eq 10 with the correspond-

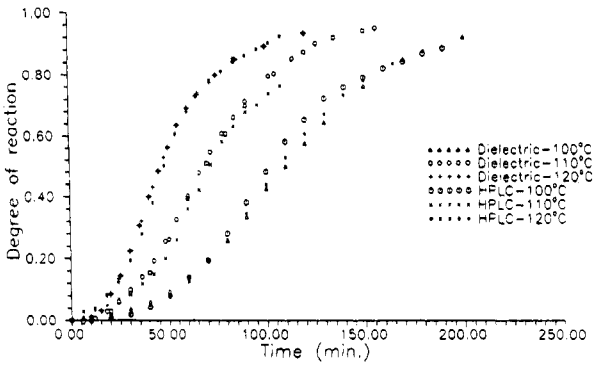

Figure 15. Comparison of the extent of reaction as a function of time for the PGE/aniline system at several temperatures, calculated from dielectric measurements and HPLC.

ing boundary conditions (eqs 11a and 11b), we obtain:

$$\frac{\alpha}{\alpha_m} = \frac{\log \varrho - \log \varrho_0}{\log \varrho_m - \log \varrho_0} \tag{12}$$

Equation 12 was then used to calculate the extent of reaction from the dielectric data. The results for PGE/aniline reaction at 100, 110, and 120 °C are shown in Figure 15. The extent of reaction was also calculated from high-performance liquid chromatography (HPLC) data[11] and plotted together with the dielectric value in Figure 15. The observed agreement between the results generated by the two techniques is remarkable!

IV. Conclusions

A reactive stoichiometric mixture of phenyl glycidyl ether and aniline was prepared and investigated by dielectric measurements in the frequency range from 20 Hz to 1 MHz and at temperatures between 90 and 120 °C. We have shown that, at frequencies where polarization by migrating charges dominates the dielectric response, the complex impedance can be used as an efficient measure of changes in the reactive system. We further conclude that the complex impedance is a versatile real-time diagnostic tool which varies systematically during reaction, is extremely reproducible and reliable, can be applied to virtually any reactive system, can be evaluated by different analytical representations, resembles qualitatively the chemorheological changes in the system, and is conducive to the development of models based on equivalent circuitry. The extents of reaction calculated from dielectric measurements and HPLC were in excellent agreement. It was concluded that the measured dielectric response, its phenomenological nature notwithstanding, can be used to follow the progress of reaction. A realization of the full potential of the analysis described in this paper, however, necessitates that fundamental correlations be developed between the dielectric response and the chemorheological changes in the reactive systems.

References and Notes

(1) McCrum, N. G.; Read, B. E.; Williams, G. *Anelastic and Dielectric Effects in Polymeric Solids*; Wiley: New York, 1967.
(2) Karasz, F. E., Ed. *Dielectric Properties of Polymers*; Plenum Press: New York, 1972.
(3) Hedvig, P. *Dielectric Spectroscopy of Polymers*; Adam Hilger: Bristol, U.K., 1977.
(4) Williams, G. *Adv. Polym. Sci.* **1979**, *33*, 60.
(5) MacCallum, J. R., Vincent, C. A., Eds. *Polymer Electrolyte Reviews 1*; Elsevier Applied Science: London, 1987.
(6) Ku, C. C.; Liepins, R. *Electrical Properties of Polymers*; Hanser: Munich, 1987.
(7) Owen, J. In *Comprehensive Polymer Science*; Allen, G., Bevington, J. C. Eds.; Pergamon Press: Oxford, U.K., 1988; Vol. 2, Chapter 21.
(8) Williams, G. In *Comprehensive Polymer Science*; Allen, G., Bevington, J. C., Eds.; Pergamon Press: Oxford, U.K., 1988; Vol. 2, Chapter 18.
(9) Riande, E.; Saiz, E. *Dipole Moments and Birefringence of Polymers*; Prentice-Hall: New York, 1992.
(10) Mijovic, J.; Kenny, J. M.; Maffezzoli, A.; Trivisano, A.; Bellucci, F.; Nicolais, L. *Comput. Sci. Technol.* **1993**, *49*, 277.
(11) Mijovic, J.; Fishbain, A.; Wijaya, J. *Macromolecules* **1992**, *25*, 979.
(12) Jonscher, K. *Phys. Status Solidi* **1975**, *32*, 665.
(13) Zukas, W. X. *Macromolecules* **1993**, *26*, 2390.
(14) Parthun, M. G.; Johari, G. P. *Macromolecules* **1993**, *26*, 2392.
(15) Sluyters-Rehbach, M.; Sluyters, J. H. In *Electroanalytical Chemistry*; Bard, A. J., Ed.; Marcel Dekker: New York, 1977; Vol. 4.
(16) Walter, G. W. *Corrosion Sci.* **1986**, *26* (9), 681.
(17) Macdonald, J. R. *Impedance Spectroscopy*; Wiley: New York, 1987.
(18) Archer, W. I.; Armstrong, R. D. *Electrochemistry*; The Royal Society of Chemistry: London, 1980; Vol. 7, p 157.
(19) Bellucci, F.; Valentino, M.; Nicodemo, L.; Kenny, J. M.; Nicolais, L.; Mijovic, J. Impedance Spectroscopy of Reactive Polymers. 1. *J. Polym. Sci., Polym. Phys. Ed.* **1994**, *32* (15), 2519.
(20) Bellucci, F.; Valentino, M.; Monetta, T.; Nicodemo, L.; Kenny, J. M.; Nicolais, L.; Mijovic, J. Impedance Spectroscopy of Reactive Polymers. 2. Multifunctional Epoxy/Amine Formulations. *J. Polym. Sci., Polym. Phys. Ed.*, in press.
(21) Keinle, R. H.; Race, H. H. *Trans. Electrochem. Soc.* **1934**, *65*, 87.
(22) Nass, A. K.; Seferis, J. C. *Polym. Eng. Sci.* **1989**, *29* (5), 315.
(23) Kenny, J. M.; Trivisano, A. *Polym. Eng. Sci.* **1991**, *31*, 19.